

Supplementary Methods

Flow Cytometry

Human. When stimulated for cytokines staining, PBMC were incubated at 37°C with PMA (50 ng/mL), ionomycin (1 µg/mL) for 5 hours. Brefeldin A (10 µg/mL) was added in the medium after 1 hour of incubation. Fc block (BD Biosciences) was used to saturate Fc receptors. First, cells were stained with a Live/Dead Fixable Yellow dye (Invitrogen) to exclude dead cells, then for extracellular markers. Intracellular staining of transcription factors, cytokines and intracellular markers was performed using the Transcription Factor Staining Buffer Set (eBioscience). Antibodies and clones are listed in Supplementary materials. Samples fluorescence was acquired with a LSR II (BD Biosciences) using FACSDiva (BD Biosciences), then analysed on FlowJo v.10 (BD Biosciences).

Mouse. For phenotypic analysis of CD8⁺ Tregs, cells were stimulated or not with PMA (50 ng/mL) and ionomycin (1 µg/mL) for 4 hours in presence of brefeldin A (10 µg/mL). Cells were stained for CD25, GITR, CD45RA, CD44, CD62L and LAP. Cells were further fixed and permeabilized using the Transcription Factor Staining Buffer Set (eBioscience), and stained with anti-FOXP3, anti-IL17 and anti-IFNγ mAbs. The fluorescence was measured with a FACS Canto II flow cytometer (BD Biosciences) and FlowJo software was used to analyze data.

Cells isolation

Human Peripheral Blood Mononuclear Cells (PBMC) were isolated from fresh blood samples with a Ficoll gradient according to the manufacturer's guidelines (Eurobio). Erythrocytes and platelets were removed with hypotonic solution and centrifugation. PBMC were then frozen at -80°C in fetal bovine serum (FBS) with 10% Dimethylsulfoxide (DMSO) and then transferred in liquid nitrogen for longer preservation. For experiments, frozen PBMC were thawed at 37°C and immediately washed with 50 mL RPMI medium with 10% FBS.

Mouse cells were collected from C57BL6 mice. Spleens and lymph nodes were homogenized, filtered through a 100 μ m cell strainer and erythrocytes were lysed. CD8⁺CD45RC^{neg} cells were obtained by fluorescence –activated cell sorter (FACS) ARIA II (BD Biosciences, Mountain View, CA) sorting based on lymphocyte morphology, living cells (Dapi⁻), dendritic and NK cells exclusion (CD11c⁻ and NK1.1⁻), CD8⁺ and CD45RC^{neg} (DNL-1.9 clone) expression. CD4⁺ regulatory or effector T cells were FACS-sorted (ARIA II, BD Biosciences) on CD11c⁻ NK1.1⁻ CD4⁺ CD25⁺ or CD11c⁻ NK1.1⁻ CD4⁺ CD25⁻ phenotype respectively. APCs were isolated from Balb/C spleens by collagenase D digestion and FACS-sorted based on lack of CD3 expression.

CNS-infiltrating cells were harvested and stained for congenic markers (CD45.2 recipient and CD45.1 donor) specific antibodies and analyzed by flow cytometry.

Expansion protocol of mouse cells.

CD8⁺ CD45RC^{neg} cells were seeded at 10⁵ in 100 μ L per well in 96-well flat-bottom plates in complete RPMI 1640 medium supplemented with 10% FBS, penicillin (100 U/mL), streptomycin (0.1 mg/mL), sodium pyruvate (1mM), L-glutamine (1mM), HEPES buffer (10 mM), nonessential amino acids (1X), 50 μ M β -mercaptoethanol, IL-2 (1,000 U/mL) and IL-15 (20 U/mL), rapamycin (50nM) and anti-CD3 and anti-CD28 mAbs coated beads at a 2:1 ratio bead:cell. IL-2 and IL-15 cytokines were freshly added in culture medium every two days, and fresh medium was added when required. Cells were harvested after 7 days of expansion as previously described ³⁵.

DGE-seq analysis

Samples expressing less than 5000 genes were excluded. Transcriptomic data were scaled by a normalization factor. Dispersion and fold-change were estimated using an empirical Bayes shrinkage procedure using DESeq2. Gene differential expression (DE) analysis was performed using a Wald

Test, with a cut-off set to zero, then corrected for multiple-testing using a Benjamini and Hochberg procedure (adjusted p-value<0.05).

Regarding analysis of biological pathways, gene set enrichment analysis (GSEA) was run for each compared cell subset, using the R package Clusterprofiler. Three databases, Gene Ontology (GO), the Kyoto Encyclopedia of Genes and Genomes (KEGG) and REACTOME were combined to identify differences of biological pathway representations (p<0.05).

Correlation between gene expression and Multiple Sclerosis Severity Score

Correlation between gene expression and the Multiple Sclerosis Severity Score (MSSS) was calculated using RStudio. Only genes associated with an absolute Pearson correlation coefficient equal or over 0.5 ($|r| \geq 0.5$) were considered. A Linear regression model was performed on each selected gene. Graphs representations of genes correlation with a p-value <0.01 using a Wald test were generated from RStudio v.1.1.477 (R v.3.3.1).

EAE

Mice were scored according to the following scale: 0, no disease; 0.5, tip of tail is limp; 1, tail paralysis; 1.5, hind leg inhibition; 2, hind limb weakness; 2.5, dragging of hind legs; 3, hind limb paralysis; 3.5, hind legs are together on one side of body; 4, fore limb weakness; 4.5, fore limb paralysis; 5, moribund or dead.

etable 1: Anti-human conjugated-antibodies used for flow cytometry

Marker	Fluorochrome	Clone	Manufacturer
2B4 (CD244)	PE	2_69	BD Biosciences
BTLA (CD272)	BV421	J168-540	BD Biosciences
CD103	BV421	Ber-ACT8	BD Biosciences
CD122	PeCy7	TU27	BioLegend
CD127	BV605	HIL-7R-M21	BD Biosciences
CD154	BV605	24-31	BioLegend
CD15s	BV711	CSLEX1	BD Biosciences
CD160	PE	BY55	BD Biosciences
CD161	BV510	HP-3G10	BioLegend
CD25	BV711	2A3	BD Biosciences
CD28	BV 421	CD28.2	BD Biosciences
CD3	APC-Cy7	SK7	BD Biosciences
CD4	PerCPCy5,5	RPAT4	BD Biosciences
CD45RC	FITC	MT2	Mast Diagnostic
CSF-1 (M-CSF)	PE	# 26786	R&D Systems
CTLA-4 (CD152)	BV605	BNI3	BioLegend
CXCR3 (CD183)	BV605	G025H7	BioLegend
Foxp3	AF647	259D/C7	BD Biosciences
GITR (CD357)	PECy7	108-17	BioLegend
IFNg	PE CF594	B27	BD Biosciences
IL-10	BV711	JES3-9D7	BD Biosciences
IL-34	PE	# 578416	R&D Systems
KLGR1	BV785	2F1/KLRG1	BioLegend
LAG3 (CD223)	PECy7	11C3C65	BioLegend
PD1 (CD279)	PeCy7	EH12	BD Biosciences
TGFβ1	PE CF594	TW4-9E7	BD Biosciences

TIM3 (CD366)	PeTr	7D3	BD Biosciences
Vα7,2	BV510	3C10	BioLegend

Table 2. Demographic and clinical characteristics of Multiple Sclerosis patients and controls

	Total		MLR	
	RR MS (n=56)	HV (n=52)	RR MS (n=30)	HV (n=24)
Female	50	43	27	22
Age (years)				
Median	38.5 ±9.8	36 ±8.68	36 ±9.52	35.5 ±10.02
range	20-58		20-55	21-56
Treatment	none	none	none	none
Disease duration				
Median	6		6	
range	1-25		1-25	
EDSS				
Median	2 ±1.72		2 ±1.8	
range	0-7.5		0-7.5	
MSSS				
Median	2.9 ±2.85		3.5 ± 3.07	
range	0.17-9.38		0.17-9.18	
ARMSS				
Median	4.2 ±2.6		4.8 ±2.77	
range	0.2-9.3		0.5-9.3	

RR MS: Relapsing Remitting Multiple Sclerosis; MLR: Mixed Lymphocyte Reaction; MSSS: Multiple Severity Score;

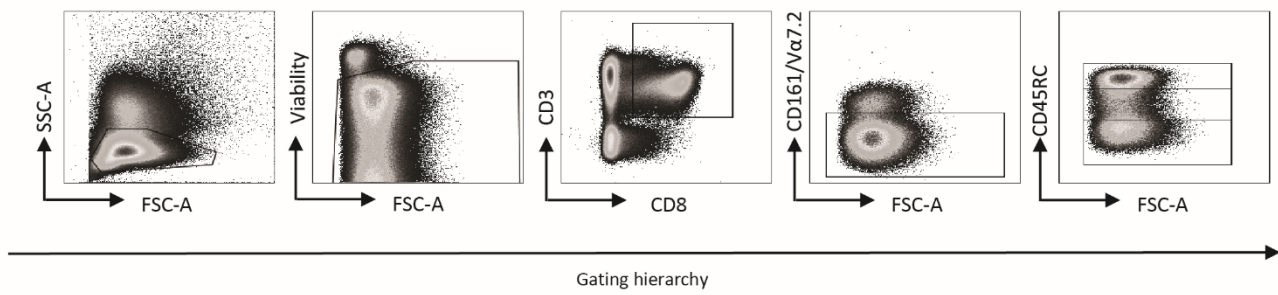
EDSS: Expanded Disability Status Scale; ARMSS: Age-Related Multiple Sclerosis Severity Score.

eTable 3. CD8⁺CD45RC^{low} gene transcripts correlating with MSSS. Only genes associated with an absolute Pearson correlation coefficient equal or over 0.5 ($|r| \geq 0.5$) were considered. A Linear regression model was performed on each selected gene. Gray-highlighted genes are positively associated with the MSSS while gene shown with a white font have a decreased expression with higher MSSS.

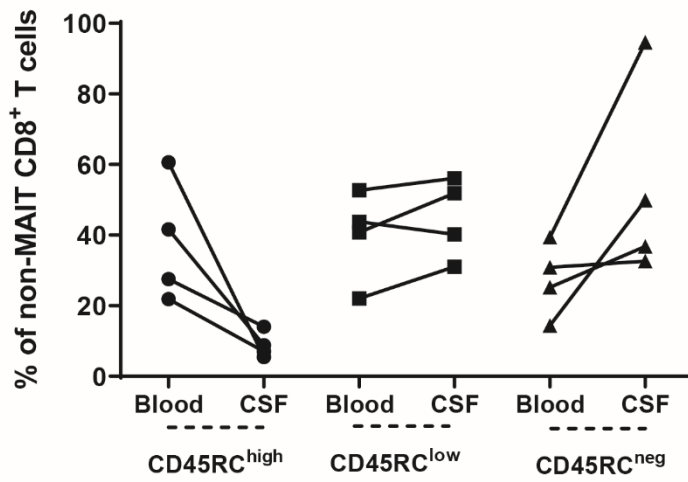
Gene	α	adjusted r^2	p-value
Cell growth and differentiation			
TBC1D7	0.13031741	0.39127255	0.00567397
Proteasome and MHC I Ag presentation			
ERAP2	0.21557394	0.34955859	0.00936045
HECTD3	-0.11295478	0.37211319	0.00716557
Cell receptors and carriers			
PROK2	0.19575155	0.58533141	0.00033552
NIPAL3	-0.094075	0.55561461	0.00055512
PIEZO1	-0.1474468	0.5159285	0.00103756
MFSD9	-0.10014459	0.41875506	0.0040142
OPRM1	-0.11333208	0.35093326	0.00921128
Transcription			
SMG8	0.13504268	0.41942601	0.00397973
ZNF696	0.08436364	0.407752	0.00461842
LITAF	0.08105611	0.38616012	0.00604223
TAF1A-AS1	0.08376289	0.37869474	0.00661805
NCOA4	0.08293757	0.3752797	0.00689732
ZNF419	0.07249335	0.36501539	0.0078008
HINFP	-0.13429603	0.43602284	0.00320602
SMARCC2	-0.08451682	0.43124249	0.00341393
FDXACB1	-0.12648766	0.42683934	0.00361587
PRMT2	-0.12383514	0.41915935	0.0039934
ZNF626	-0.11128668	0.4154079	0.00419015
ELL3	-0.12589663	0.41226772	0.00436137
FAM102A	-0.15891156	0.40544039	0.00475512
FAM153C	-0.13258685	0.40286778	0.00491145
FARSA	-0.0971409	0.39247722	0.00559015
POU2F2	-0.15298565	0.39041605	0.00573424
DCP2	-0.06859035	0.38153142	0.00639376
UPF2	-0.07878531	0.36089543	0.00819206
TCF7	-0.15551784	0.35638827	0.00864002
Signal transduction			
STRAP	0.0718788	0.40111099	0.0050208
DPP4 = CD26	-0.14960591	0.45019984	0.00265345
STAMBP	-0.07798012	0.44305711	0.00292035
DUSP16	-0.16814968	0.44274624	0.00293248
MAL	-0.22263829	0.41968254	0.00396662
PDE8A	-0.12319972	0.38778476	0.00592297
GNAS	-0.06385879	0.37973307	0.00653516
C6orf25 = G6B	-0.08238081	0.37208509	0.00716799
PTCHD4	-0.09600184	0.36276173	0.00801271
NFKB1	-0.13766975	0.35582244	0.00869777
DNA replication and repair			

POLR3C	0.10473711	0.44278452	0.00293099
SPIDR	-0.16092415	0.44626654	0.00279763
NOC3L	-0.14895751	0.36178913	0.00810574
Cellular stress response			
GPX1	-0.13894759	0.41698525	0.0041064
TRAP1	-0.10737051	0.3930359	0.00555165
Membrane trafficking			
SRGN	0.12073707	0.44173013	0.00297245
GCA	-0.12325114	0.37552532	0.00687689
RTN3	-0.14535893	0.35595059	0.00868466
Cell cycle			
CDC14A	-0.15558986	0.40863646	0.00456705
CCNY	-0.13957062	0.34893209	0.00942914
Cytoskeleton			
COTL1	-0.08368444	0.47050499	0.00200807
MYO15B	-0.11554536	0.45728071	0.00241028
CCDC14	-0.17097438	0.41898156	0.00400254
NF2	-0.17554961	0.36408647	0.00788753
Mitochondrial energetic metabolism			
NADK2	0.13974229	0.3923335	0.00560009
AKAP1	-0.12271238	0.40820518	0.00459204
PTCD2	0.07703507	0.4056559	0.00474223
Lipid metabolism			
FDPS	0.08265531	0.41349869	0.00429352
HDLBP	-0.18128667	0.389792	0.00577851
Others			
C8orf86	0.09511371	0.5752889	0.00039922
ZFPL1	0.15921838	0.47468832	0.00189377
ZSCAN30	0.13703071	0.42397564	0.00375279
ERLEC1	-0.07576499	0.50315242	0.00125626
DPH3P1	-0.12150312	0.37835482	0.00664539
ZC3H13	-0.09610527	0.3746123	0.00695311
ADHFE1	-0.12565437	0.35925016	0.00835313
FGFR1OP2	-0.08728032	0.34687589	0.00965777
PTAR1	-0.16178861	0.34558947	0.00980331

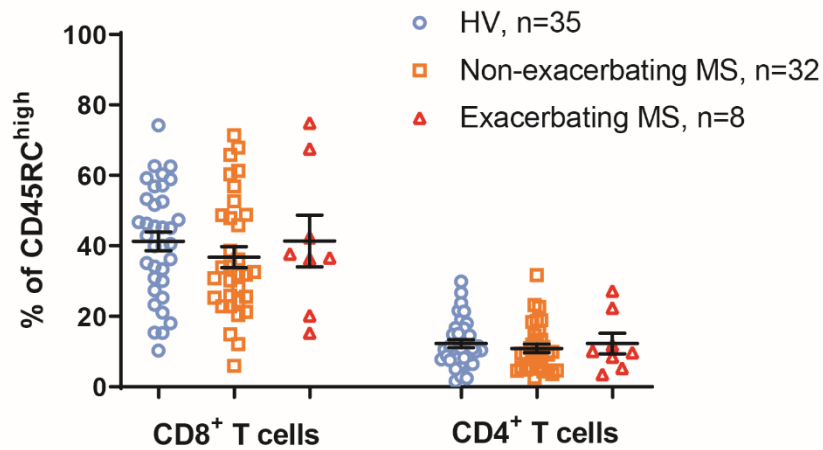
A



B

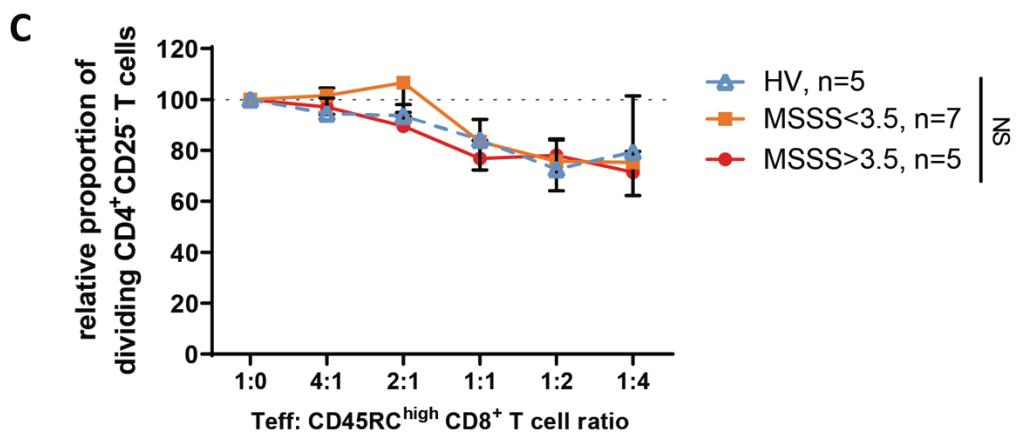
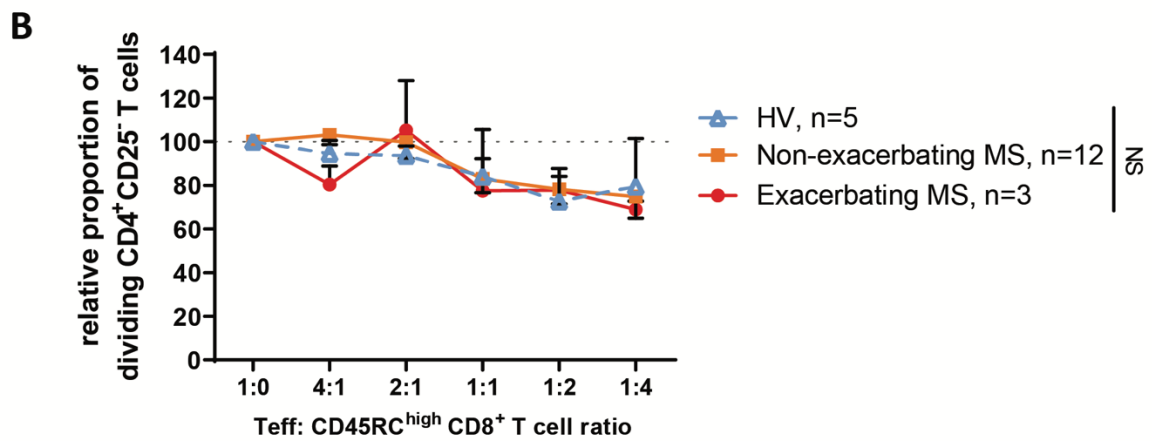
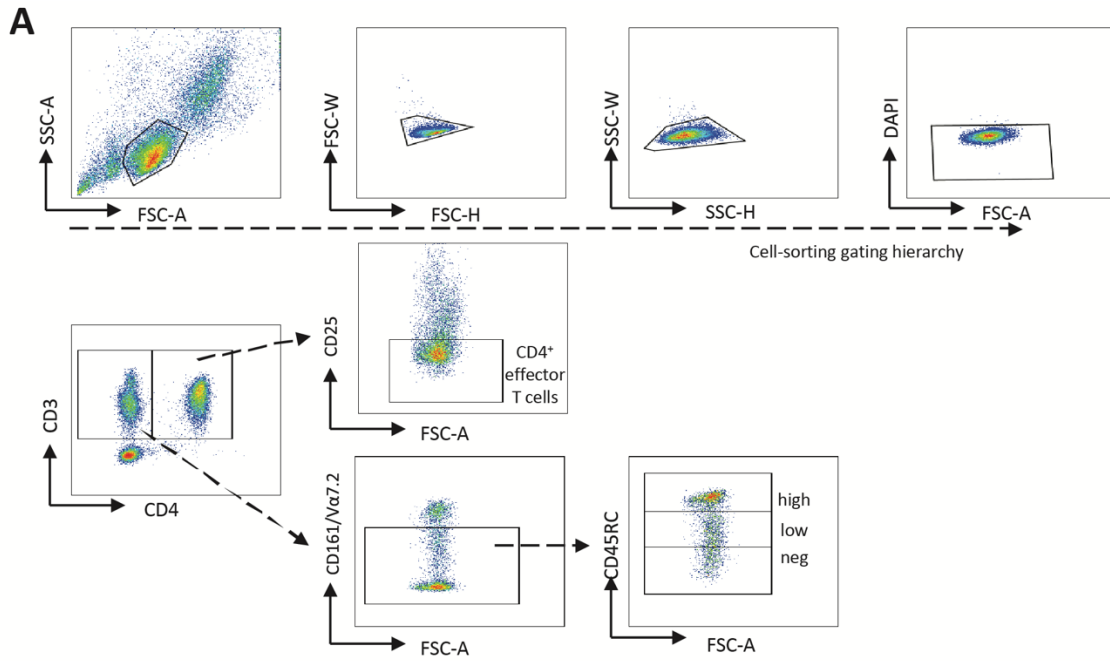


C

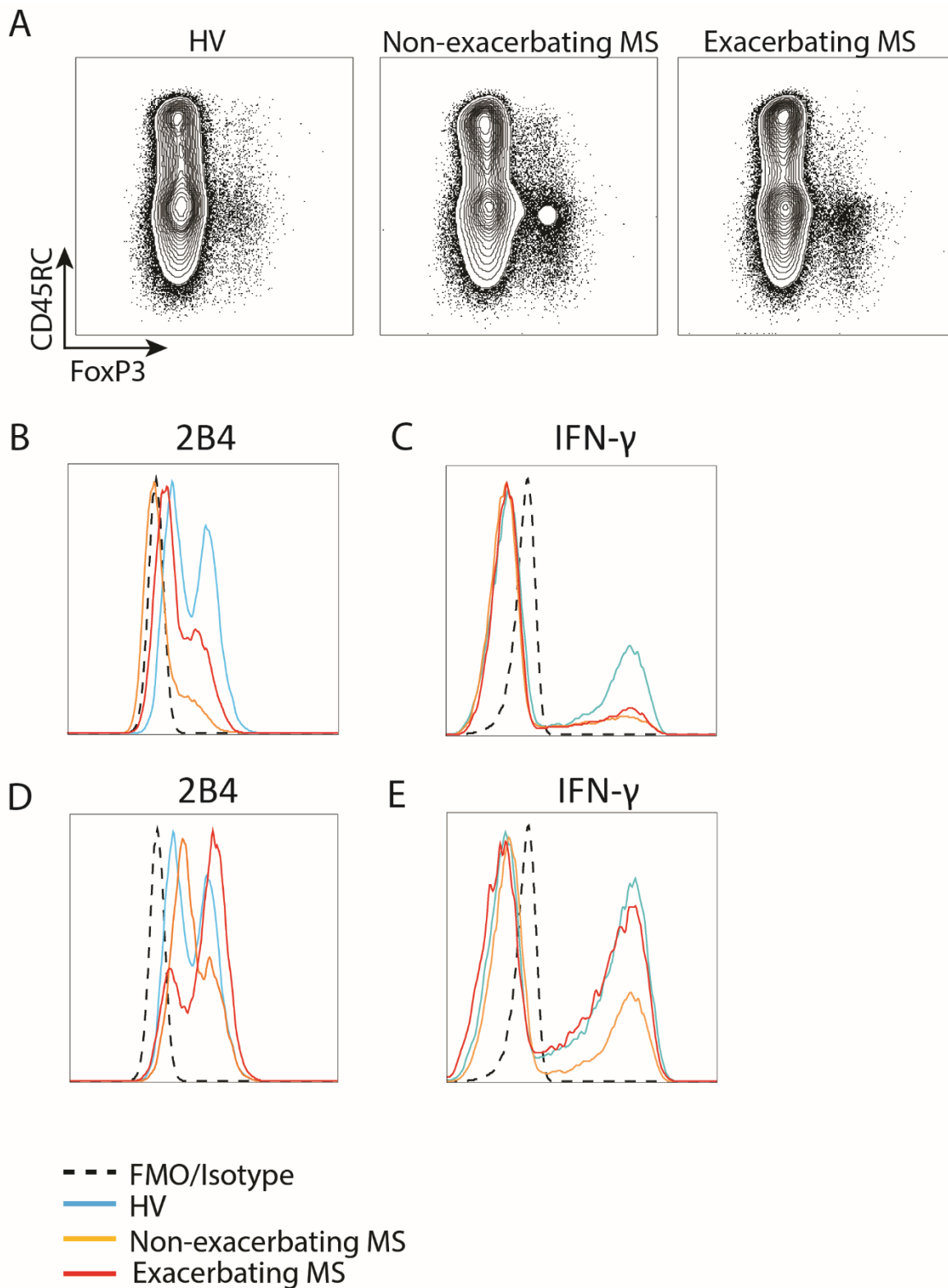


eFig. 1. CD45RC marker frequency in non-CNS inflammatory neurological controls and MS patients. (A) Flow cytometry strategy to define the CD8⁺CD45RC subsets. Cells were gated on morphology, SSC and FSC singlet, living cells, CD3⁺, CD8⁺, CD161^{low/neg} TCRVα7.2^{low/-} to exclude MAIT cells respectively, CD3⁺, CD8⁺ and were subdivided into three subsets depending on CD45RC

marker expression to define $CD45RC^{high}$, $CD45RC^{low}$, $CD45RC^{neg}$ subsets respectively. The $CD45RC^{low/neg}$ population comprises both $CD45RC^{low}$ and $CD45RC^{neg}$ cell subsets. **(B)** Frequency of non-MAIT $CD8^{+}CD45RC$ cell subsets in blood and CSF of non-CNS inflammatory neurological controls. Match-paired frequencies, $n=4$. Statistical analysis was performed using Wilcoxon signed-rank test. **(C)** Frequency of $CD45RC^{high}$ cells in $CD8^{+}$ and $CD4^{+}$ T cells subsets in MS patients in exacerbating and non-exacerbating MS patients vs HV. Statistical analysis was performed using Kruskal-Wallis test adjusted with Dunn's test.

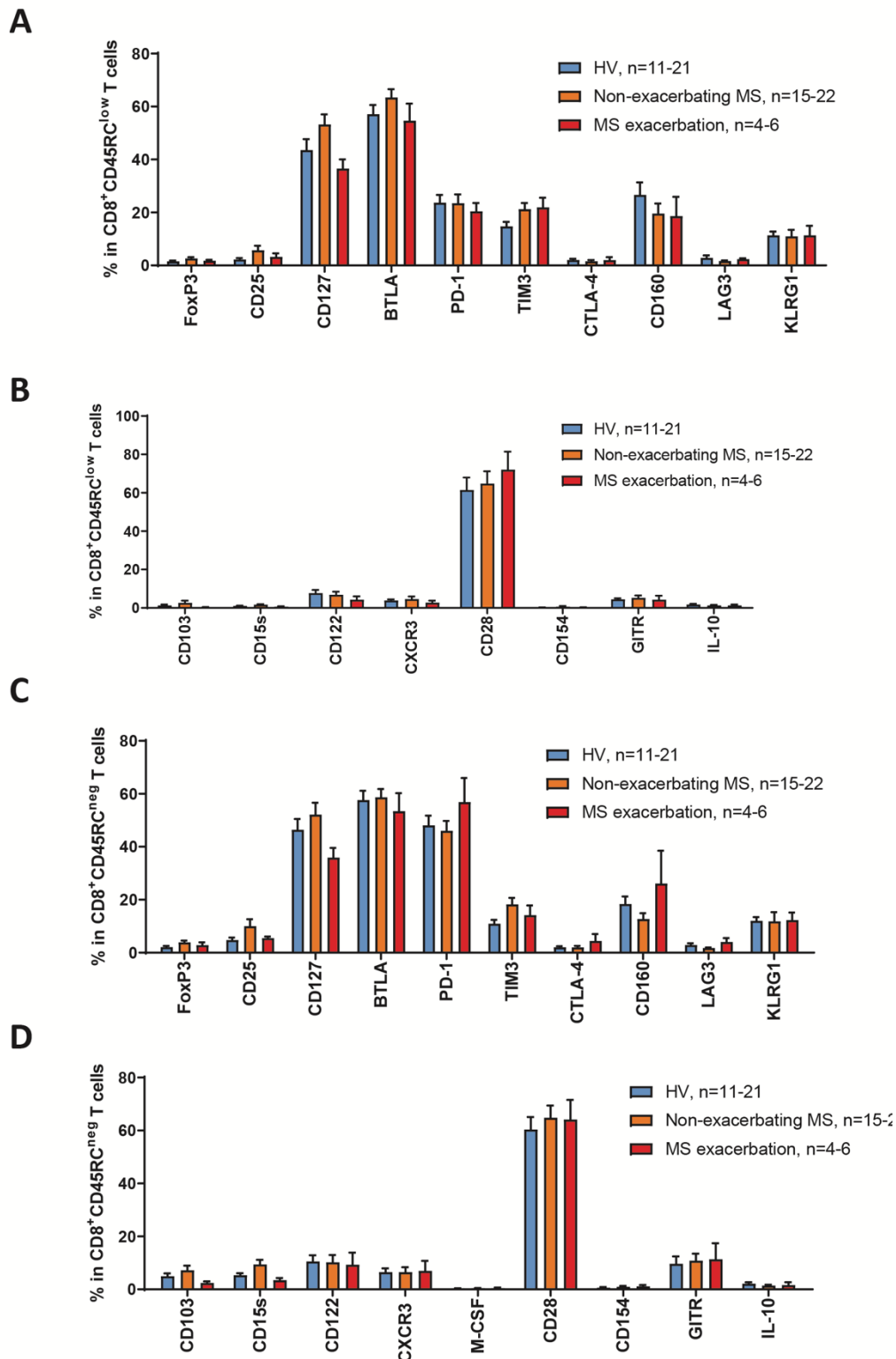


eFig. 2. CD8⁺CD45RC^{high} T cells do not suppress effector T cell proliferation. (A) CD8⁺ T cell subsets were sorted on morphology, then FSC and SSC singlets, living cells, CD3⁺, CD4⁺, CD161^{low/neg} TCRV α 7.2^{low/neg} to exclude MAIT cells and were subdivided into three subsets depending on the high, low or negative expression of the CD45RC marker. Conventional effector T cells were sorted on morphology, then FSC and SSC singlets, living cells, CD3⁺, CD4⁺, CD25⁻ and labeled with CFSE. (B) CD8⁺CD45RC^{high} T cells from HV (n=5; blue) and non-exacerbating (n=12; orange) and exacerbating (n=3; red) MS patients (B) or from MSSS<3.5 (n=7; orange) and MSSS>3.5 (n=5; red) non-exacerbating MS patients (C) were added in an ascending ratio to CFSE-labeled CD4⁺CD25⁻ T cells (Teff) stimulated with allogeneic APCs. Proliferation of was assayed by flow cytometry after 5-days culture. Statistical analysis was performed using two-way ANOVA corrected for multiple comparison with a Bonferroni test. NS: not significant. Teff: effector T cells.



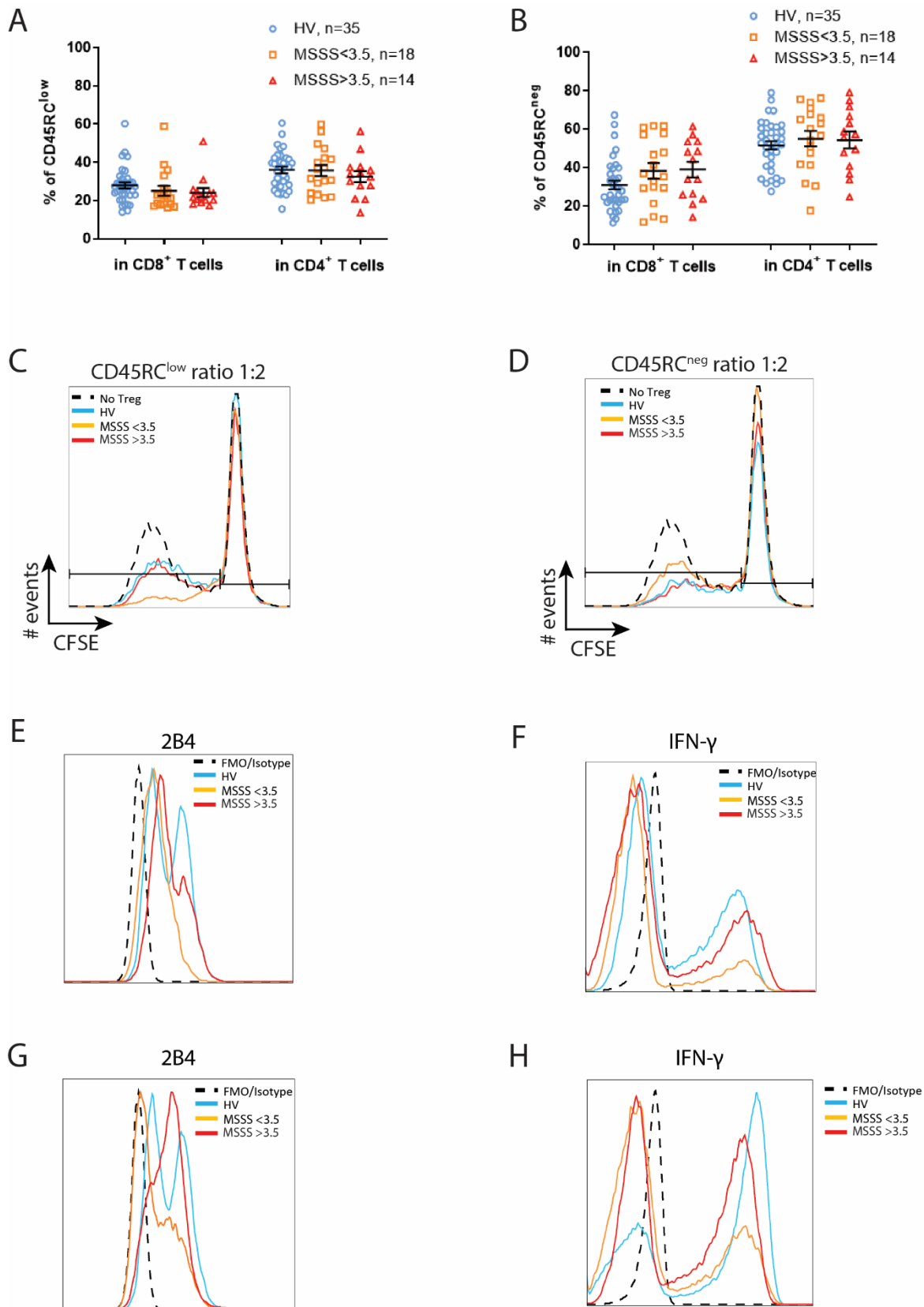
eFig. 3. Representative flow plots of CD8⁺CD45RC^{low} and CD45RC^{neg} subsets according to patient exacerbation status. **A.** Representative flow cytometry plot of fluorescence intensity of CD45RC and FoxP3 within CD3⁺CD8⁺CD161^{low/neg} TCRV α 7.2^{low/-} cells in HV, non-exacerbating and exacerbating MS patients. **B-E.** Representative flow cytometry plot of fluorescence intensity of

2B4 and IFN- γ within blood CD3⁺CD8⁺CD161^{low/neg}TCRV α 7.2^{low/-} cells in CD8⁺CD45RC^{low} (**B** and **C**) and CD8⁺CD45RC^{neg} (**D** and **E**) cells respectively in both HV (blue), non-exacerbating (orange) and exacerbating (red) MS patients. FMO was used for extracellular markers and isotype controls for intracellular staining. FMO: focal minus one.



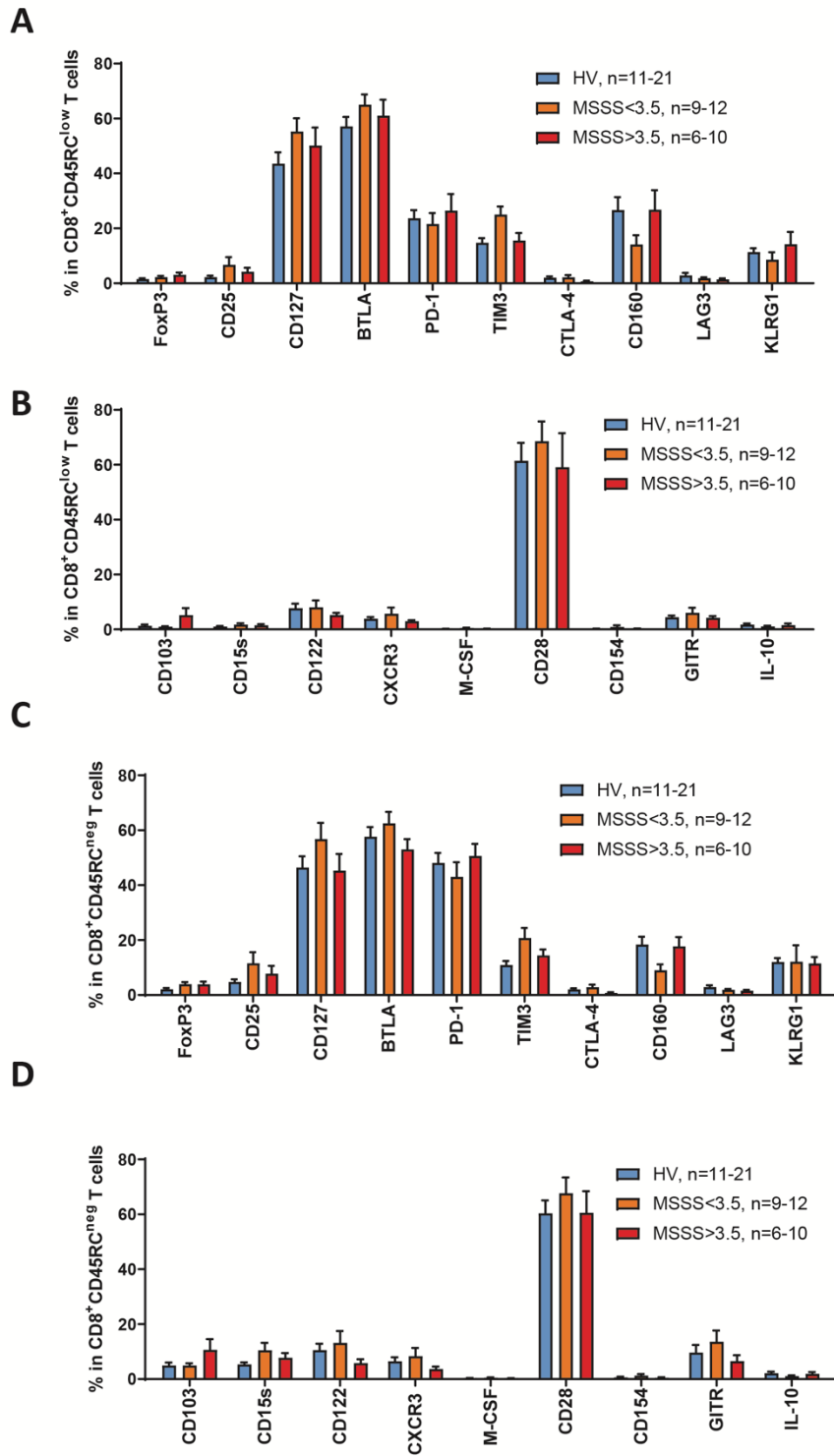
eFig. 4. Markers expressed by CD8⁺CD45RC^{low} and CD8⁺CD45RC^{neg} T cells in MS patients not impacted by exacerbation. A-D. Activation, regulatory and exhaustion markers were analyzed by flow cytometry, without (A and C) or following (B and D) 5h of PMA-ionomycin stimulation as indicated, in CD8⁺CD45RC^{low} (A and B) or CD8⁺CD45RC^{neg} T cells (C and D) of HV (blue-colored)

and non-exacerbating (orange) vs exacerbating (red) MS patients. Results are shown as mean \pm SEM. Statistical analysis was performed using two-way ANOVA corrected for multiple comparison with a Bonferroni test.



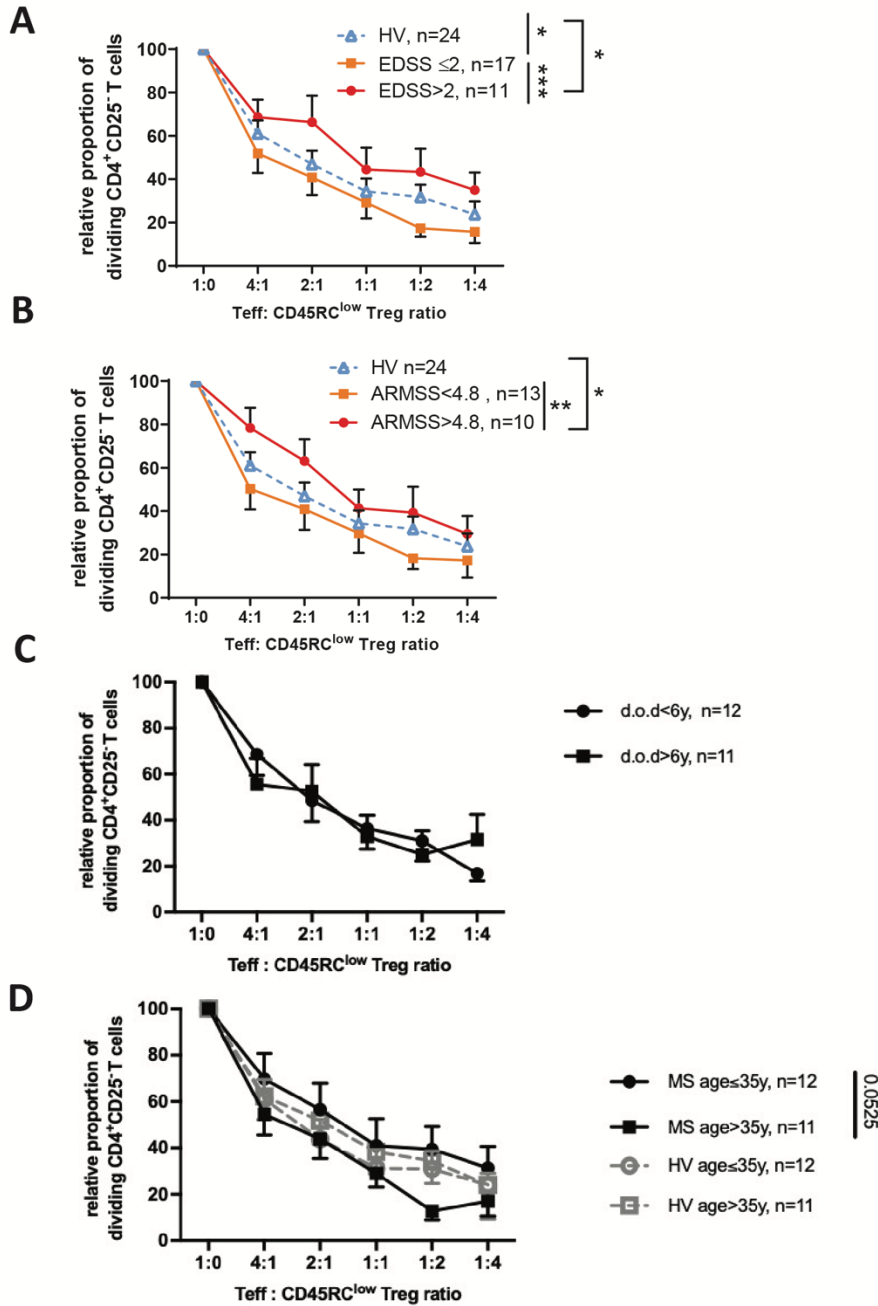
eFig. 5. Representative flow plots of CD8⁺CD45RC^{low} and CD45RC^{neg} subsets according to patient exacerbation status. A, B. Frequency of CD45RC^{low} (A) and CD45RC^{neg} (B) in blood CD4⁺ and CD8⁺ T cells from MS patients according to MS severity based on a Multiple Sclerosis

Severity Score (MSSS) below (orange) or above (red) 3.5 and in HV (blue). Statistical analysis was performed using a Kruskal-Wallis test adjusted with a Dunn's test. **C,D**. Representative histograms illustrate CFSE fluorescence intensity featuring Teff proliferation for each group, CD8⁺CD45RC^{low} (**B**) and CD8⁺CD45RC^{low} (**D**) respectively, at the 1:2 Teff:Treg ratio (dashed black line represents the 1:0 ratio). **E-H**. Representative flow cytometry plot of fluorescence intensity of 2B4 and IFN- γ within blood CD3⁺CD8⁺CD161^{low/neg} TCRV α 7.2^{low/-} cells in CD8⁺CD45RC^{low} (**E** and **F**) and CD8⁺CD45RC^{neg} (**G** and **H**) cells respectively in both HV (blue), mild (orange) and severe (red) MS patients according to the MSSS. FMO was used as a control of extracellular markers and isotype controls for intracellular staining (dashed line). *FMO: focal minus one. MSSS: Multiple Sclerosis Severity Score.*



eFig. 6. Markers expressed by CD8⁺CD45RC^{low} and CD8⁺CD45RC^{neg} T cells not impacted by disease severity. A-D. Activation, regulatory or exhaustion markers were analyzed by flow cytometry, without (A and C) or following (B and D) 5h of PMA-ionomycin stimulation as indicated, in CD8⁺CD45RC^{low} (A and B) or CD8⁺CD45RC^{neg} T cells (C and D) of HV (blue) and MSSS below

3.5 (orange) vs MSSS above 3.5 (red) MS patients. Results are shown as mean \pm SEM Statistical analysis was performed using two-way ANOVA corrected for multiple comparison with a Bonferroni test.

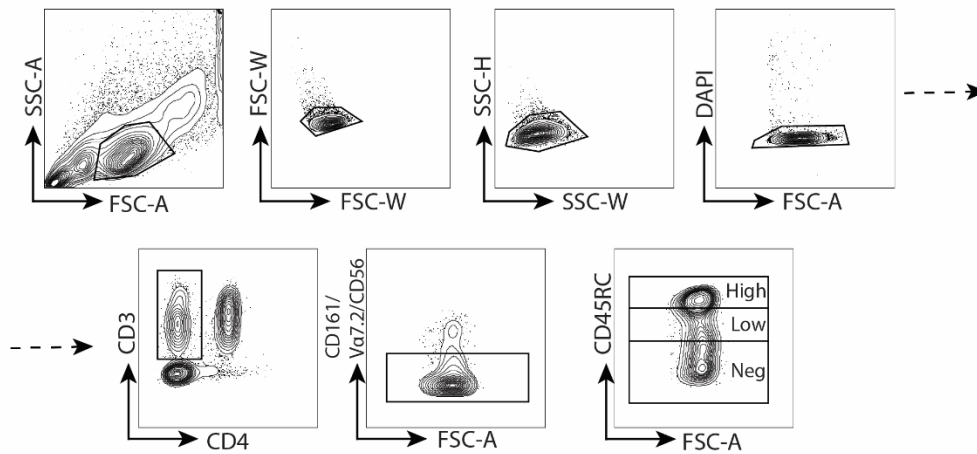


eFig. 7. Suppressive activity of CD8⁺CD45RC^{low} was lost in patient with high EDSS or age-related MS scores but not correlated with duration of disease or age of MS patients.

The suppressive ability of CD8⁺CD45RC^{low} cells was evaluated in patients with **(A)** a moderate or severe disability (EDSS >2) (n=7; red) as compared to patients with milder symptoms (EDSS ≤2) (n=16; orange) and HV (n=24; blue), **(B)** an Age-Related-Multiple Sclerosis Severity score (ARMSS) below 4.8 (n=13; orange), median of the cohort, compared to a higher ARMSS (n=10; red) score and HV (n=24; blue), **(C)** different duration of disease (d.o.d) using a threshold of 6 years corresponding

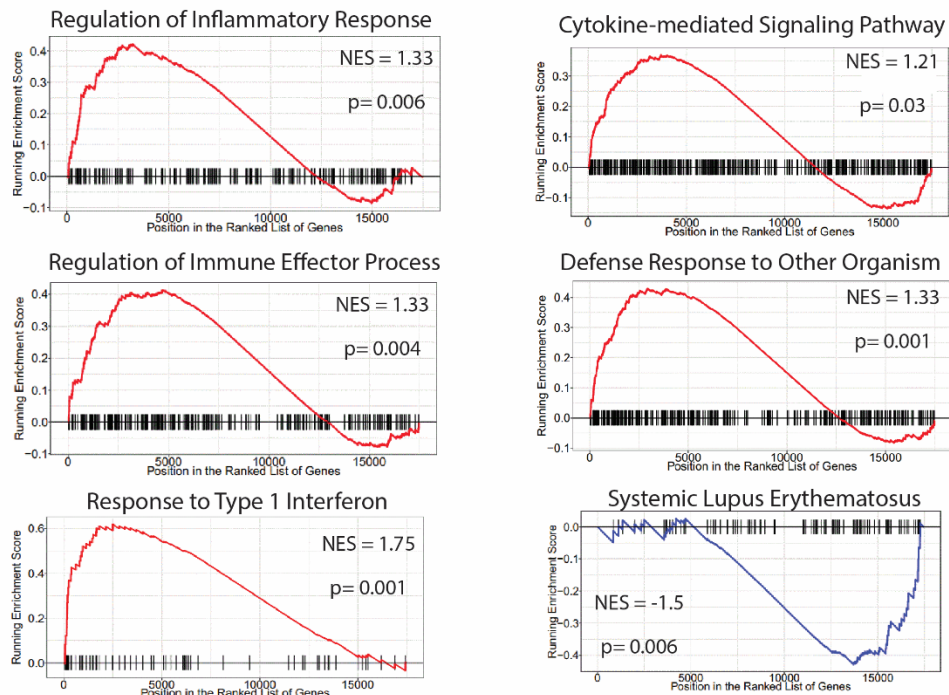
to the median of disease length in the cohort (n=12 and n=11) or **(D)** a threshold of 35 years of age, median of the cohort, to segregate groups. Statistical analysis was performed using two-way ANOVA. * $p<0.05$; ** $p<0.01$; *** $p<0.001$. Mean \pm SEM.

A



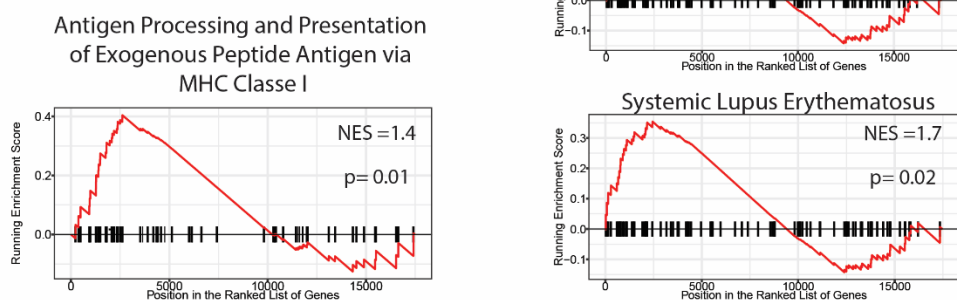
B

CD8⁺CD45RC^{low} MSSS <3.5 versus >3.5



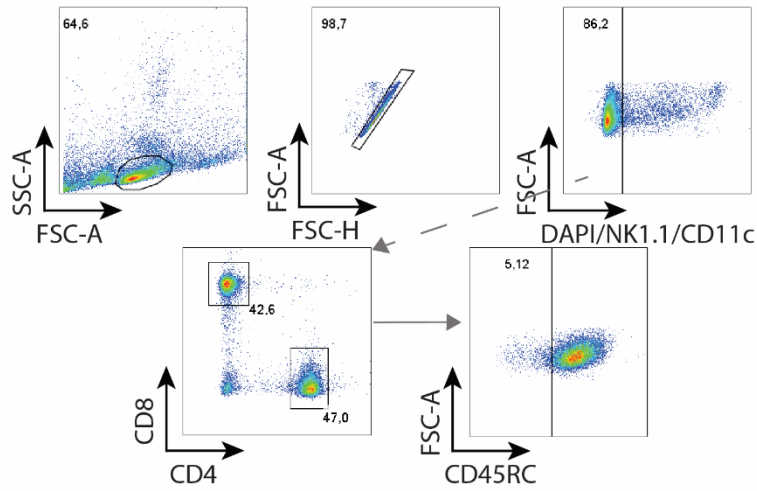
C

CD8⁺CD45RC^{low} MSSS >3.5 versus HV

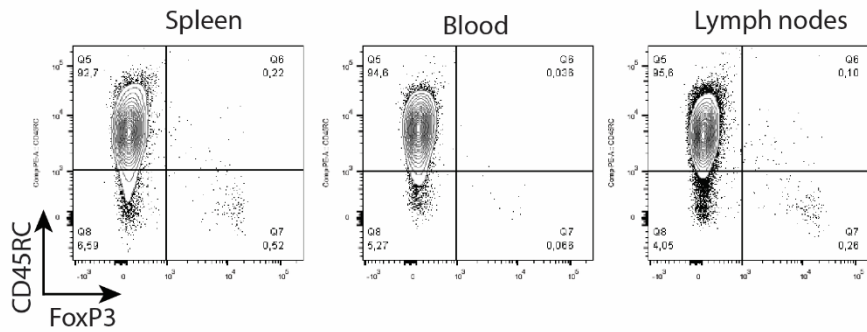


eFig. 8. Transcriptomic analysis of CD8⁺CD45RC^{low} cells of severe and milder form of MS revealed differentially expressed pathways. A. Flow cytometry gating strategy to sort out the CD8⁺CD45RC subsets for DGE-sequencing. Cells were gated on morphology, then FSC and SSC singlets, living cells, CD3⁺, CD8⁺, CD161^{low/neg} TCR V α 7.2^{low/neg} and CD56^{low/neg} to exclude MAIT cells and NKT cells respectively, CD3⁺, CD4⁻ and were subdivided into three subsets depending on the high, low or negative expression of the CD45RC marker. **B, C.** Representative GSEA plots of CD45RC^{low} from MS patients with a MSSS<3.5 (n=10) versus MSSS>3.5 (n=7) (**B**) and MSS>3.5 (n=7) versus HV (n=10) (**C**).

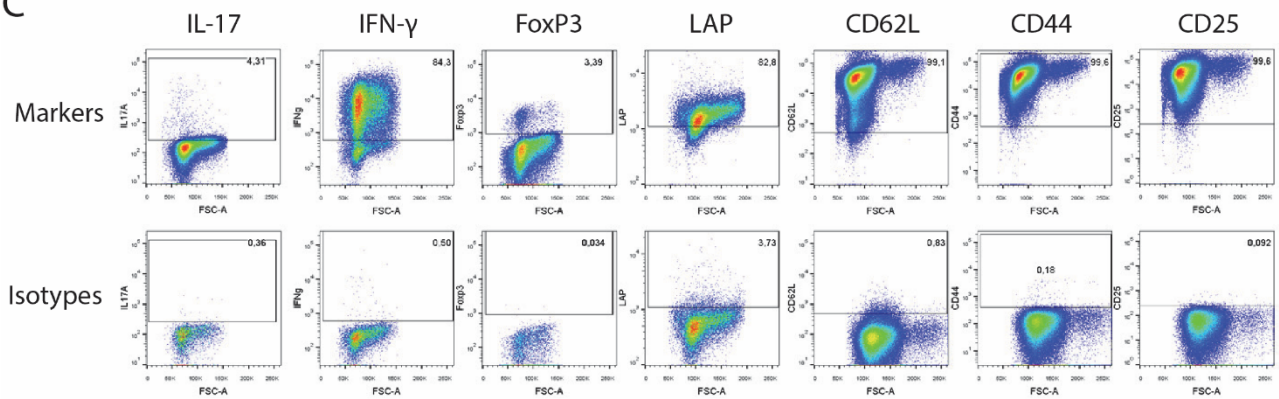
A



B



C



eFig. 9: Isolation of mouse $CD8^+CD45RC^{neg}$ Tregs before expansion. **A.** Gating strategy for $CD8^+CD45RC^{neg}$ Tregs sorting by FACS Aria from splenocytes. $CD8^+$ Tregs were selected on morphology, exclusion of doublets, dead cells, $NK1.1^+$, $CD11c^+$ and $CD4^+$ cells, positive selection of $CD8^+$ and $CD45RC^{neg}$ expression. **B.** Representative flow cytometry plot of fluorescence intensity of $CD45RC$ and $FoxP3$ within murine $CD8$ T cells according to gating strategy depicted in (A). **C.**

Representative staining for expression of activation and exhaustion markers or cytokines and Treg-associated markers after a 4h PMA-ionomycin stimulation of expanded CD8⁺ CD45RC⁻ Tregs were analyzed.